

Structural characterization of polymeric nanofibers of polyvinylidene fluoride (PVDF)

José Augusto Souza Gomes da Silva¹ , Wallace Rodrigues da Silva Júnior² ,
Ana Neilde Rodrigues da Silva³ , Roseli Künzel⁴ , José Roberto Ribeiro Bortoleto² ,
Emanuel Benedito de Melo⁵ , Carina Ulsen⁶  and Neilo Marcos Trindade^{7*} 

¹*Programa de Pós-graduação em Engenharia Mecânica, Instituto Federal de Educação, Ciência e Tecnologia, São Paulo, Brasil*

²*Programa de Pós-graduação em Ciência e Tecnologia de Materiais, Universidade Estadual Paulista “Júlio de Mesquita Filho”, São Paulo, Brasil*

³*Departamento de Sistemas Eletrônicos, Faculdade de Tecnologia do Estado de São Paulo, São Paulo, Brasil*

⁴*Departamento de Física, Universidade Federal de São Paulo, São Paulo, Brasil*

⁵*Departamento de Física, Instituto Federal de Educação, Ciência e Tecnologia, Itapetininga, Brasil*

⁶*Laboratório de Caracterização Tecnológica, Escola Politécnica, Universidade de São Paulo, São Paulo, Brasil*

⁷*Instituto de Física, Universidade de São Paulo, São Paulo, Brasil*

*neilotrindade@usp.br

Abstract

Polyvinylidene fluoride (PVDF) is a polymer material that exhibits piezoelectricity, which is the ability of certain materials to generate an electric charge in response to applied mechanical stress. Electrospun nanofibers were prepared from a solution with 1800 mg PVDF (18 wt.%) powder dissolved in 7.5 ml of dimethylformamide (DMF) and 2.5 ml acetone. The experimental setup used in the electrostatic deposition process was developed in our laboratory. Atomic Force Microscopy (AFM) showed that the fibers vary from 100 nm to 200 nm. Scanning Electron Microscopy (SEM) measurements showed distributed and well-formed nanofibers, but with few incidences of beads. The Energy Dispersive Spectroscopy (EDX) results showed that all points of the formed nanofibers have very similar chemical compositions, based on carbon and fluorine. Raman and Fourier Transform Infrared (FTIR) Spectroscopic analysis revealed the characteristic bands related to β -phase in the sample, which is responsible for the piezoelectricity of PVDF.

Keywords: *beta phase, electrospinning, nanofibers, piezoelectricity.*

How to cite: Silva, J. A. S. G., Silva Júnior, W. R., Silva, A. N. R., Künzel, R., Bortoleto, J. R. R., Melo, E. B., Ulsen, C., & Trindade, N. M. (2023). Structural characterization of polymeric nano-fibers of polyvinylidene fluoride (PVDF). *Polímeros: Ciência e Tecnologia*, 33(1), e20230011. <https://doi.org/10.1590/0104-1428.20220117>

1. Introduction

Polyvinylidene fluoride (PVDF) has drawn much attention in the scientific, technological, and industrial community due to its good mechanical properties, resistance to acids, solvents, heat, radiation, and low cost^[1,2]. However, other characteristics considered more relevant are the high ferroelectric, pyroelectric, piezoelectric, and dielectric response^[2-5]. This polymer consists of alternating CH₂ and CF₂ groups along its polymer chain. In addition, the polymer can crystallize into, at least, five distinct crystalline phases, known as alpha (α), beta (β), gamma (γ), delta (δ), and epsilon (ϵ)^[6-12]. Each phase provides unique properties to the polymer and, therefore, different applications^[13,14]. The α -phase is the most common crystalline phase obtained by PVDF. This phase is non-polar and can be obtained by cooling solutions with different solvents, for example, dimethylformamide (DMF)^[15]. The β -phase is the one with the highest dipole moment and highest piezoelectric response; therefore, it is

the most desirable for various applications^[5]; for example, for applications in sensors and actuators, as it displays better pyro- and piezoelectric properties^[4,16]. Recently, it was found that in the crystallization of PVDF from a solution in DMF, the α or β phases can be obtained, depending on the chosen crystallization temperature^[17]. PVDF solution concentration is usually used within a range of 10 – 25 wt.%^[2,4]. At high and low PVDF concentrations, there are no stability in β -phase formation and fewer entanglements between polymer molecular chains, respectively^[2]. The PVDF nanofibers were obtained by electrospinning.

Electrospinning is one of the most versatile techniques for obtaining fibrous structures with diameters in micro and nanometer scales^[4,18-20]. Electrospinning is a technique that uses electrostatic forces to produce fibrous filaments with diameters in the micrometer and nanometer scale^[21-23]. This

technique has received considerable attention due to the low cost of the materials involved, easy assembly, and handling^[4].

Over the years, researchers related to the subject have shown that, due to their high surface/volume ratio and high performance, electrospun fibers could have great potential in various applications^[19]. The properties of the materials used in the process can be promoted in the electrospun fibers, which can act, *e.g.*, as chemical protective clothing^[24], biomedicine^[25], filtering process^[26,27], sensors^[4,28], electronic devices^[26,29,30], etc. However, for the transfer of this technology to industry and large-scale production, it has been necessary to overcome some limitations such as (i) low fiber deposition rate, (ii) production of fibers with controlled and consistent diameters, and (iii) the obtaining fibers free of defects inherent to the control of process parameters^[31]. To overcome these issues, modifications are being carried out in the process and there is a great deal of research focused on evaluating the parameters that influence the execution of the technique, whether they are related to the properties of the solution, environmental conditions of the electrospinning system or inherent to the process itself^[23,32].

Within this context, this work presents the production of PVDF fibers in concentration of 18 wt.% and their physical-chemical characterization by atomic force microscopy, energy dispersive X-ray analysis, scanning electron microscopy, Raman and FTIR spectroscopy. In our laboratory, the homemade system is used to produce the nanofibers.

2. Materials and Methods

2.1 Materials

Electrospun nanofibers were prepared from a solution of PVDF powder dissolved in DMF and acetone. The polymer concentration was determined by the percentage of PVDF mass (mg) in the solvent volume (ml). The solution was prepared with 1800 mg of PVDF (18 wt.%), 2.5 ml of acetone, and 7.5 ml of DMF. For the total dissolution of the polymer, a magnetic stirrer at 900 RPM was used for 2 hours. The PVDF ($M_w = 534,000 \text{ g}\cdot\text{mol}^{-1}$) and DMF

(>98%) were purchased from Sigma-Aldrich. Acetone (99.8%) was purchased from MERCK.

2.2 Experimental setup

Figure 1a shows the experimental setup employed in the electrostatic deposition process. The process consists of three steps: (i) completely dissolving the polymer in an appropriate solvent to form a polymer solution of suitable viscosity; (ii) placing the resulting solution in a capillary; and (iii) subjecting the solution to a potential difference^[33,34]. With the application of high voltage DC, an electric field is created between the capillary (which contains the solution with the polymer dissolved in a suitable solvent) and the collector plate^[21]. In setting up the experimental arrangement, one of the terminals of the high voltage source is connected to the syringe needle and the other is connected to the metallic base or collector. When a potential difference is applied, a polarization is created and then the solution droplets are attracted by the electric field to the collector, which contains the neutral potential of the connected high voltage source. The electric field formed contributes to the appearance of electrostatic and drag forces that act on the polymer solution^[21]. The initial flow can be given by gravity, a metering pump, or by the process handler. When the applied electric field is sufficient to break the attraction forces between the molecules of the solution, the liquid is expelled in the form of a jet of fibers^[19,23,35].

The system is composed of a plastic box, a high voltage DC source variable from 0 to 30 kV and 0.400 mA, machined polypropylene support with a rod used to fix syringes from 3 ml to 10 ml^[36]. In this system, height can vary from 0 to 35 cm, and the angular inclination of the syringes varies from 0 to 360°. A grounded metallic plate was also used where the fiber deposition was concentrated. The distance between the tip of the 22G1 hypodermic needle (25.0×0.7 mm) and the metallic base was set at 15 cm. The hypodermic needle inclines approximately 320° relative to the horizontal, and for this procedure, the needle tip was previously cut and sanded to increase the outflow of the polymer solution. Based in previous results, the electrical potential difference

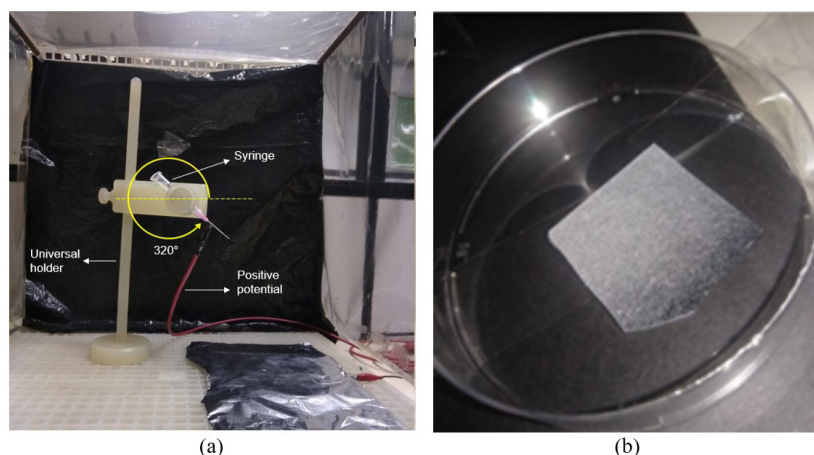


Figure 1. (a) Homemade electrospinning system; (b) monocrystalline silicon wafer cleaved with deposited fibrous material.

was set at 15 kV^[33]. The duration of the electrospinning was 3 minutes at room temperature. The box was developed with plastic material to ensure electrical isolation and favor the electrospinning process, also avoiding, for example, air currents to interfere in the formation of field lines and consequently the direction of fibers to the sample. In addition, the plastic box offers greater safety to the operator, as it does not allow contact with the solvent that evaporates from the electrospun fibers^[36]. The syringe containing the solution was adequately connected to the positive pole of the high voltage source, while the metallic collector was connected to the ground of the high voltage source. It was not necessary to use the syringe plunger, because the initial flow of the process was spontaneously established due to the gravitational action and the viscosity of the solution. The electrospun fibers were collected over the metallic collector covered by monocrystalline silicon cleaved into small squares measuring 1.5×1.5 mm as shown in Figure 1b.

2.3 Characterization techniques

Atomic force microscope (AFM) analysis was performed to identify the fibers morphology and roughness using the XE-100 Park Systems. The analysis was performed in non-contact mode using a silicon tip with a nominal radius of 5 nm over a scanning area of 8 μm² for 2D images. The scanning electron microscope (SEM) was also employed to analyze the morphology. Energy dispersive X-ray (EDX) analysis was used to characterize the elements and their distribution. For SEM and EDX analysis, the FEI Quanta 650 FEG was used. As the electrospun fiber is a polymeric material, a thin platinum layer with approximately 10 nm was sputtered over the sample in order to increase the conductivity and allow the electron dissipation.

Raman spectroscopy was used to provide molecular information and the phase composition was investigated

using Fourier Transformed Infrared (FTIR). Raman spectra were recorded in a Renishaw microscope (InVia model) with a multichannel CCD detector and He-Ne laser (632.8 nm). The Raman spectra were recorded in the range from 100 to 3200 cm⁻¹ with the cosmic ray removal option on. FTIR spectra were registered on a Shimadzu (IEPrestige-21) spectrophotometer. A pellet technique was used with potassium bromide (KBr) which is transparent to the radiation. The fibers were scrapped from the silicon surface added to KBr powder and pressed until a pellet is formed. The FTIR spectra were obtained with 120 scans and in the region between 400 and 1400 cm⁻¹.

3. Results and Discussions

Figure 2a shows an AFM image of 5×5 μm. It can be observed several nanofibers on Si substrate. Figure 2b shows a 1D AFM profile at the position of the dashed line. The radius of the nanofibers varies from 100 nm to 200 nm as estimated by AFM analysis. In particular, the typical radius for the electrospun nanofiber is 150 nm as shown in Figure 2c. These value are in agreement with reported previously in the literature^[37,38]. In addition, it was also possible to verify that during the scan of the nanofibers, the AFM tip came across a bead and then the profile drawn in the graph did not follow the curvature expected in the projections of the other nanofibers. Therefore, the difference between the fiber radius observed in the AFM analysis confirms the influence of the solutions parameter. Finally, Figure 2d shows a 3D representation of the AFM image shown in Figure 2a.

Figure 3a presents morphological images of PVDF sample on the substrate obtained from SEM. In addition, Figure 3b-3c show the detail of the surface and the interior of a bead, which is rounded structure that forms along with

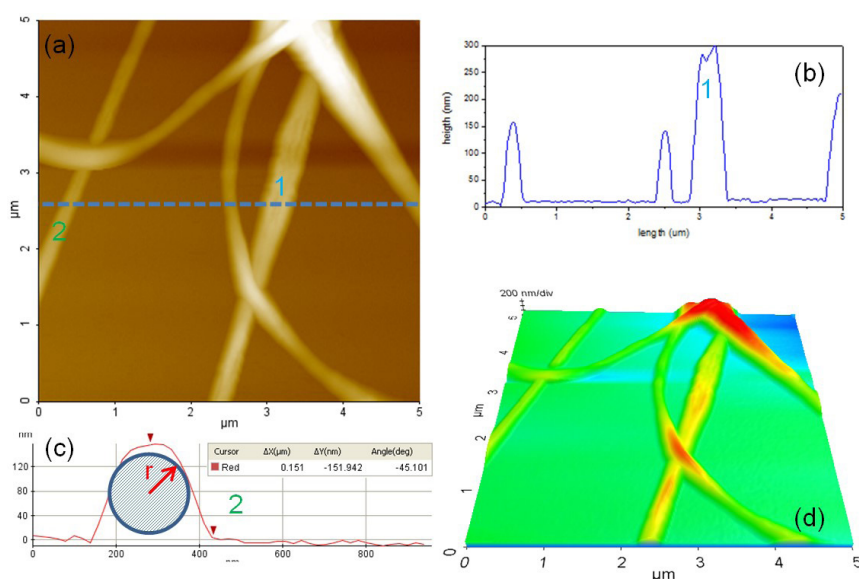


Figure 2. (a) AFM image of 5×5 μm containing typical nanofibers; (b) 1D AFM profile at the position of the dashed line. It is possible to notice that when the radius of the nanofibers exceeds 150 nm, can occur self-deformation; (c) 1D AFM profile of nanofiber on position 2. Nanofibers with radius up to 150 nm maintain the tubular shape; (d) 3D representation of the AFM image is shown in Figure 2a.

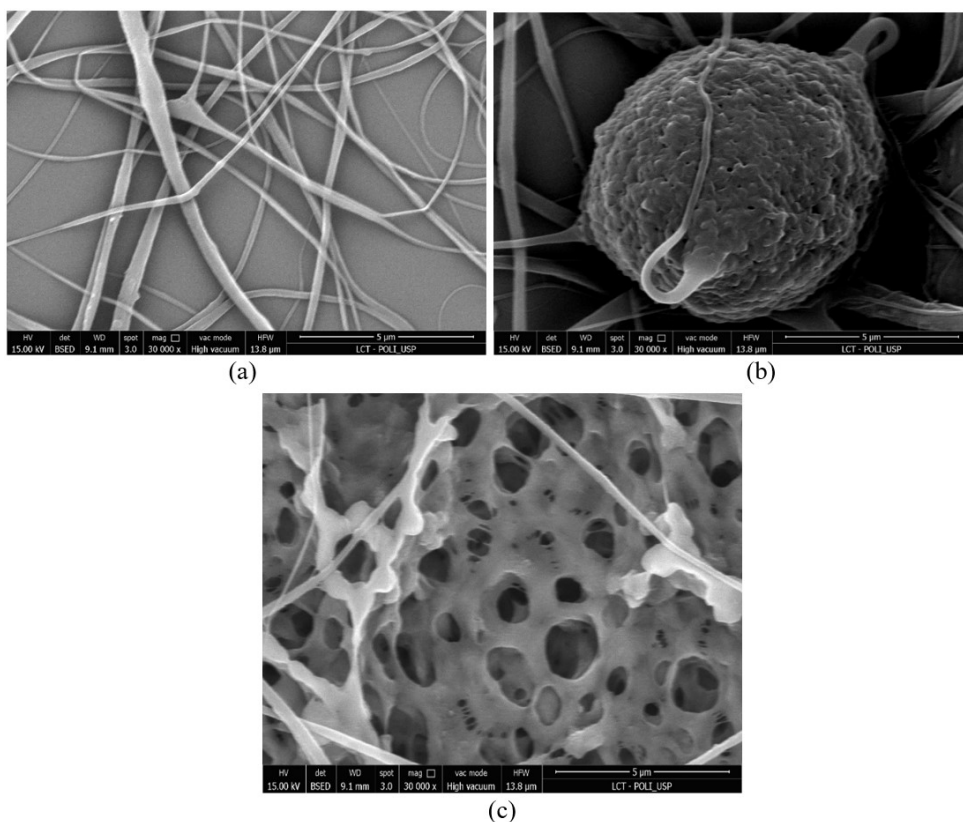


Figure 3. SEM images of PVDF sample (a) deposited on the substrate; (b) surface of a bead; (c) interior of a bead.

the fiber. Figure 3a-3b illustrates that electrospun of the fibers are randomly distributed, well-formed, and with few incidences of beads. The applied voltage was sufficient to generate an electric field capable of overcoming the surface tension of the solution and distorting the droplet until the formation of fibrous material. As the fibers were not divided into droplets before reaching the collector plate, it is verified that the polymer concentrations did not negatively influence the process. The distance between the collecting tube and the syringe and the outflow of the polymer solution through the cut and sanded needle was assertive, as the fibers generated present few imperfections, which indicates adequate evaporation of the solvent until the material deposits on the silicon blade. In addition, in Figure 3b-3c, the occurrence of the beads interferes with the linearity of fibers. This could be due to distortion in the electric field during the process. When the deposition starts, the distribution of the electric field that forms between the capillary tube and the collecting base is homogeneous, but over time the nanofibers already deposited on the surface of the material behave as an insulator, distorting and directing the jet to regions still free of deposition, in this case, the edges of the silicon wafer.

To perform the EDX analysis, six points of sample was selected and numbered (1 - 6), three in the beads (1, 2, 3) and three in the fibers (4, 5, 6), as shown in Figure 4. The EDX results showed that all points have very similar

compositions, containing carbon and fluorine, in addition to the platinum used in the coating. EDX analysis also reveals no specific or differentiated behavior regarding mapping the elemental chemical composition of beads and fibers. Overall, such imperfections in fiber linearity are related to process parameters and solution properties^[39].

The Raman spectrum of the sample is shown in Figure 5. Some authors^[30,40,41] have already described that the electrospinning process favors the appearance of the β -phase. With it in mind, it is possible to notice the presence of bands referring to the β -phase at 421 cm^{-1} , 840 cm^{-1} , and 1278 cm^{-1} in the spectrum^[13,30,40]. The band observed at 799 cm^{-1} is designed as α -phase^[12]. The peak at 840 cm^{-1} is higher in intensity than at 799 cm^{-1} , which may indicate a predominance of β -phase if compared to the α -phase. Bands referring to CH_2 , which belong to the PVDF polymer chain, are also present and occur in about 1430 cm^{-1} ^[12]. The intense peak centered around 522 cm^{-1} corresponds to scattering by optical phonons of the first order of the silicon lattice structure^[37]. The spectrum measured of a silicon standard is illustrated in the inset of Figure 5 and the main peak falls around 522 cm^{-1} . In the studied sample, the peak around 522 cm^{-1} arises from the monocrystalline silicon that covers the metallic collector where the nanofibers are deposited.

Figure 6 shows the registered FTIR spectra of the sample. Vibrational bands at 611 cm^{-1} (CF_2 bending), 763 cm^{-1} (CF_2 bending and skeletal bonding)^[10,38], and

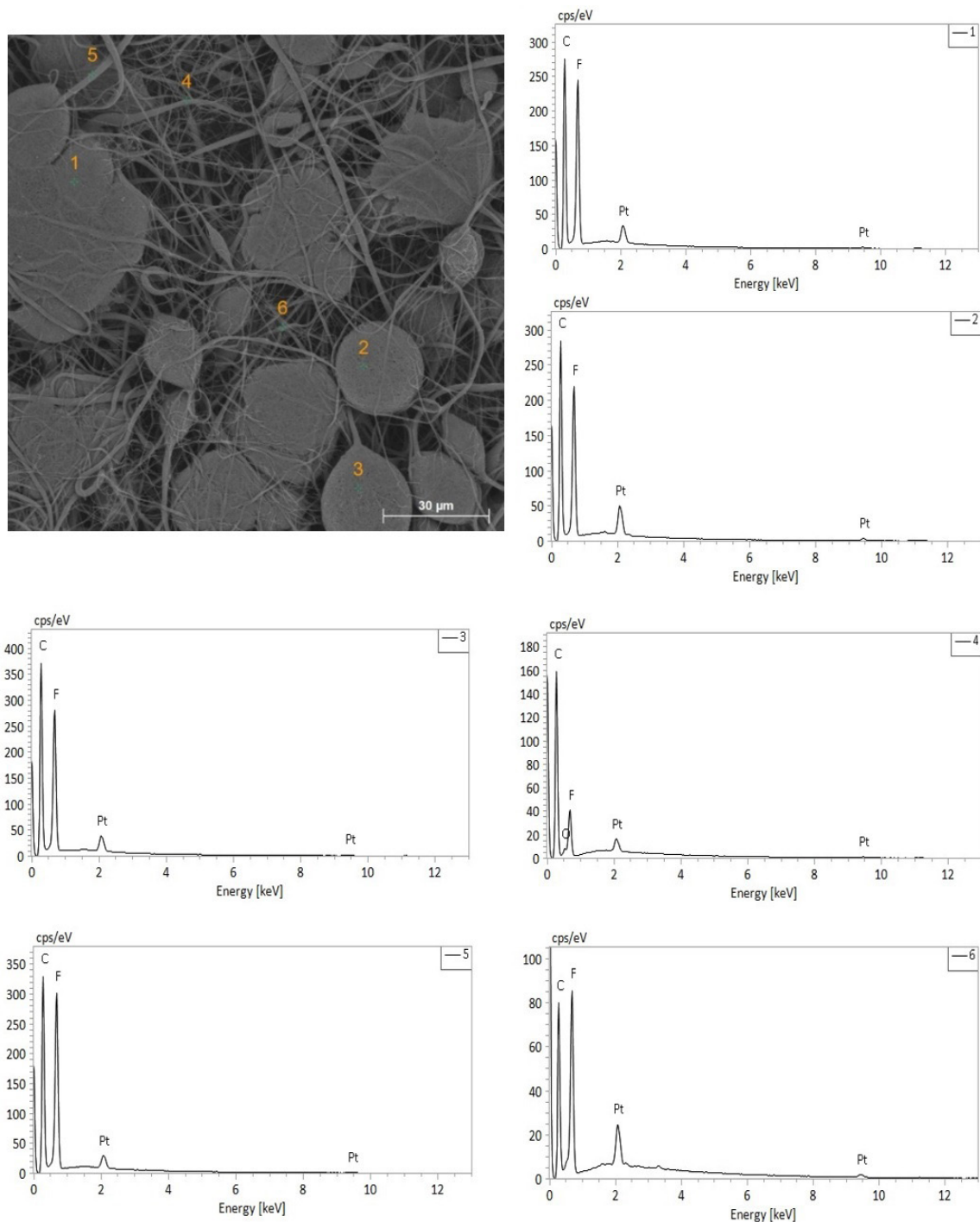


Figure 4. Selected points in PVDF sample and EDX spectrum of the six selected points.

987 cm^{-1} were identified in the spectrum of fibers, which refer to the α -phase^[13,30,40]. The characteristic bands of the β -phase, responsible for the piezoelectric properties, appear at 441 cm^{-1} , 510 cm^{-1} , 745 cm^{-1} , 840 cm^{-1} , and 1280 cm^{-1} . When one compares the peaks at 840 and 1275 cm^{-1} to that at 766 cm^{-1} , in our work (840 and 1280 cm^{-1} to that at

763 cm^{-1}), it is noticeable that most of the α -phase in the raw powder was converted to β -phase^[10]. The FTIR analysis confirm the formation of the β -phase and the bands designed for this phase are also intense and well-defined. According to literature^[9,38,42], there is no evidence of formation of γ -phase in solution.

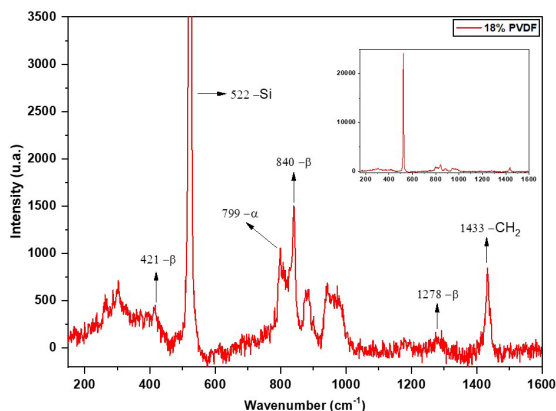


Figure 5. Raman spectrum obtained of the PVDF sample. The inset shows the spectrum measured of a silicon standard.

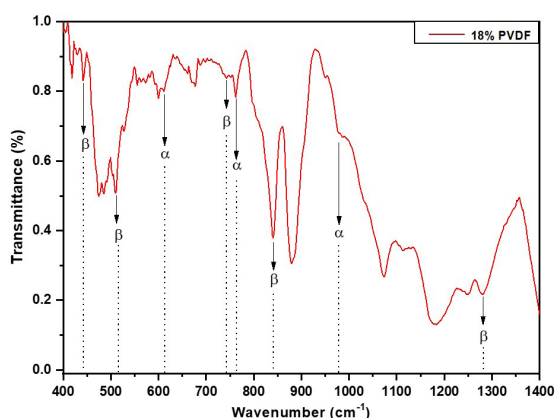


Figure 6. FTIR spectrum obtained from PVDF sample.

4. Conclusions

The solution of polyvinylidene fluoride (PVDF 18 wt.%) was explored to obtain nanofibers by electrospinning technique. For the physical-chemical characterization of these membranes; AFM, SEM, EDX, Raman, and FTIR spectroscopy techniques were used. AFM showed that the typical radius for the electrospun nanofiber was 150 nm. From SEM, sample showed few incidences of imperfections and good formation, in addition to being continuous with nanometric diameters and randomly deposited on the substrate. In addition, EDX showed the mapping that the elemental chemical composition of the beads, and the part of the fibers are similar. Raman spectroscopy and FTIR revealed information about the α , β crystalline phases, and the details of the chemical bonds in the structure of the samples. The parameters used in the synthesis (1800 mg of PVDF, 2.5 ml of acetone, and 7.5 ml of DMF); as well as in electrospinning (applied voltage of 15 kV, distance between the needle and the grounded collector of 15 cm), were assertive for the development of nanofibrous materials for application purposes as piezoelectric material.

5. Author's Contribution

- **Conceptualization** – José Augusto Souza Gomes da Silva; Ana Neilde Rodrigues da Silva; Neilo Marcos Trindade.
- **Data curation** – José Augusto Souza Gomes da Silva; Ana Neilde Rodrigues da Silva.
- **Formal analysis** – José Augusto Souza Gomes da Silva; Ana Neilde Rodrigues da Silva.
- **Funding acquisition** – Carina Ulsen; Neilo Marcos Trindade.
- **Investigation** – José Augusto Souza Gomes da Silva; Wallace Rodrigues da Silva Júnior; Ana Neilde Rodrigues da Silva; Carina Ulsen; Roseli Künzel; José Roberto Ribeiro Bortoleto; Emanuel Benedito de Melo.
- **Methodology** – José Augusto Souza Gomes da Silva; Ana Neilde Rodrigues da Silva; Neilo Marcos Trindade.
- **Project administration** – José Augusto Souza Gomes da Silva; Ana Neilde Rodrigues da Silva; Neilo Marcos Trindade.
- **Resources** – Ana Neilde Rodrigues da Silva; Carina Ulsen; Neilo Marcos Trindade.
- **Software** – NA.
- **Supervision** – Ana Neilde Rodrigues da Silva; Neilo Marcos Trindade.
- **Validation** – José Augusto Souza Gomes da Silva.
- **Visualization** – José Augusto Souza Gomes da Silva.
- **Writing – original draft** – José Augusto Souza Gomes da Silva; Wallace Rodrigues da Silva Júnior; Neilo Marcos Trindade.
- **Writing – review & editing** – José Augusto Souza Gomes da Silva; Wallace Rodrigues da Silva Júnior; Ana Neilde Rodrigues da Silva; Carina Ulsen; Roseli Künzel; José Roberto Ribeiro Bortoleto; Neilo Marcos Trindade.

6. Acknowledgements

N. M. Trindade is grateful to Fundação de Amparo à Pesquisa do Estado de São Paulo – FAPESP (#2019/05915-3) and Conselho Nacional de Desenvolvimento Científico e Tecnológico – CNPq (#409338/2021-4). W. R. S. Júnior thanks to Coordenação de Aperfeiçoamento de Pessoal de Nível Superior – CAPES. The authors are grateful to Núcleo de Instrumentação para Pesquisa e Ensino da Universidade Federal de São Paulo – NIPE-Unifesp and Faculdade de Tecnologia do Estado de São Paulo – FATEC for experimental support.

7. References

1. Martins, P., Lopes, A. C., & Lanceros-Mendez, S. (2014). Electroactive phases of poly(vinylidene fluoride): Determination, processing and applications. *Progress in Polymer Science*, 39(4), 683-706. <http://dx.doi.org/10.1016/j.progpolymsci.2013.07.006>.
2. He, Z., Rault, F., Lewandowski, M., Mohsenzadeh, E., & Salaün, F. (2021). Electrospun PVDF nanofibers for piezoelectric applications: a review of the influence of electrospinning parameters on the β phase and crystallinity enhancement.

- Polymers*, 13(2), 174. <http://dx.doi.org/10.3390/polym13020174>. PMID:33418962.
3. Nalwa, H. S. (1995). *Ferroelectric polymers*. Boca Raton: CRC Press. <http://dx.doi.org/10.1201/9781482295450>.
 4. Kalimuldina, G., Turdakyn, N., Abay, I., Medeubayev, A., Nurpeissova, A., Adair, D., & Bakenov, Z. (2020). A review of piezoelectric PVDF film by electrospinning and its applications. *Sensors*, 20(18), 5214. <http://dx.doi.org/10.3390/s20185214>. PMID:32932744.
 5. Ribeiro, C., Costa, C. M., Correia, D. M., Nunes-Pereira, J., Oliveira, J., Martins, P., Gonçalves, R., Cardoso, V. F., & Lanceros-Méndez, S. (2018). Electroactive poly(vinylidene fluoride)-based structures for advanced applications. *Nature Protocols*, 13(4), 681-704. <http://dx.doi.org/10.1038/nprot.2017.157>. PMID:29543796.
 6. Lin, Y., Zhang, Y., Zhang, F., Zhang, M., Li, D., Deng, G., Guan, L., & Dong, M. (2021). Studies on the electrostatic effects of stretched PVDF films and nanofibers. *Nanoscale Research Letters*, 16(1), 79. <http://dx.doi.org/10.1186/s11671-021-03536-9>. PMID:33939029.
 7. Pan, C.-T., Dutt, K., Yen, C.-K., Kumar, A., Kaushik, A. C., Wei, D.-Q., Kumar, A., Wen, Z.-H., Hsu, W.-H., & Shiue, Y.-L. (2022). Characterization of piezoelectric properties of Ag-NPs doped PVDF nanocomposite fibres membrane prepared by near field electrospinning. *Combinatorial Chemistry & High Throughput Screening*, 25(4), 720-729. <http://dx.doi.org/10.2174/1386207324666210302100728>. PMID:33653246.
 8. Gade, H., Bokka, S., & Chase, G. G. (2021). Polarization treatments of electrospun PVDF fiber mats. *Polymer*, 212, 123152. <http://dx.doi.org/10.1016/j.polymer.2020.123152>.
 9. Singh, R. K., Lye, S. W., & Miao, J. (2021). Holistic investigation of the electrospinning parameters for high percentage of β -phase in PVDF nanofibers. *Polymer*, 214, 123366. <http://dx.doi.org/10.1016/j.polymer.2020.123366>.
 10. Gade, H., Nikam, S., Chase, G. G., & Reneker, D. H. (2021). Effect of electrospinning conditions on β -phase and surface charge potential of PVDF fibers. *Polymer*, 228, 123902. <http://dx.doi.org/10.1016/j.polymer.2021.123902>.
 11. Dashtizad, S., Alizadeh, P., & Yourdkhani, A. (2021). Improving piezoelectric properties of PVDF fibers by compositing with BaTiO₃-Ag particles prepared by sol-gel method and photochemical reaction. *Journal of Alloys and Compounds*, 883, 160810. <http://dx.doi.org/10.1016/j.jallcom.2021.160810>.
 12. Ma, J., Zhang, Q., Lin, K., Zhou, L., & Ni, Z. (2018). Piezoelectric and optoelectronic properties of electrospinning hybrid PVDF and ZnO nanofibers. *Materials Research Express*, 5(3), 035057. <http://dx.doi.org/10.1088/2053-1591/aab747>.
 13. Costa, L. M. M., Bretas, R. E. S., & Gregorio, R. Fo. (2009). Characterization of β -PVDF films prepared at different conditions. *Polímeros: Ciência e Tecnologia*, 19(3), 183-189. <http://dx.doi.org/10.1590/S0104-14282009000300005>.
 14. Lederle, F., Härter, C., & Beuermann, S. (2020). Inducing β phase crystallinity of PVDF homopolymer, blends and block copolymers by anti-solvent crystallization. *Journal of Fluorine Chemistry*, 234, 109522. <http://dx.doi.org/10.1016/j.jfluchem.2020.109522>.
 15. Ma, W., Zhang, J., Chen, S., & Wang, X. (2008). Crystalline phase formation of poly(vinylidene fluoride) from tetrahydrofuran/N,N-dimethylformamide mixed solutions. *Journal of Macromolecular Science, Part B: Physics*, 47(3), 434-449. <http://dx.doi.org/10.1080/00222340801954811>.
 16. Nunes-Pereira, J., Costa, P., & Lanceros-Mendez, S. (2018). *Piezoelectric energy production*. In I. Dincer (Ed.), *Comprehensive energy systems* (pp. 380-415). Amsterdam: Elsevier. <http://dx.doi.org/10.1016/B978-0-12-809597-3.00324-2>.
 17. Sencadas, V., Moreira, M. V., Lanceros-Méndez, S., Pouzada, A. S., & Gregório, R. Fo. (2006). α - to β transformation on PVDF films obtained by uniaxial stretch. *Materials Science Forum*, 514-516, 872-876. <http://dx.doi.org/10.4028/www.scientific.net/MSF.514-516.872>.
 18. Garg, K., & Bowlin, G. L. (2011). Electrospinning jets and nanofibrous structures. *Biomicrofluidics*, 5(1), 13403. <http://dx.doi.org/10.1063/1.3567097>. PMID:21522493.
 19. Huang, Z.-M., Zhang, Y.-Z., Kotaki, M., & Ramakrishna, S. (2003). A review on polymer nanofibers by electrospinning and their applications in nanocomposites. *Composites Science and Technology*, 63(15), 2223-2253. [http://dx.doi.org/10.1016/S0266-3538\(03\)00178-7](http://dx.doi.org/10.1016/S0266-3538(03)00178-7).
 20. Zhang, R., Zhang, T., Cai, Y., Zhu, X., Han, Q., Li, Y., Liu, Y., Wang, A., & Lan, G. (2019). Synthesis and characterization of a spun membrane with modified Al₂O₃. *Journal of Plastic Film & Sheeting*, 35(4), 380-400. <http://dx.doi.org/10.1177/8756087919840684>.
 21. Kumar, C. N., Prabhakar, M. N., & Song, J.-I. (2021). Synthesis of vinyl ester resin-carrying PVDF green nanofibers for self-healing applications. *Scientific Reports*, 11(1), 908. <http://dx.doi.org/10.1038/s41598-020-78706-3>. PMID:33441603.
 22. Russo, F., Ursino, C., Avruscio, E., Desiderio, G., Perrone, A., Santoro, S., Galiano, F., & Figoli, A. (2020). Innovative Poly (Vinylidene Fluoride) (PVDF) electrospun nanofiber membrane preparation using DMSO as a low toxicity solvent. *Membranes*, 10(3), 36. <http://dx.doi.org/10.3390/membranes10030036>. PMID:32110883.
 23. Costa, R. G. F., Oliveira, J. E., Paula, G. F., Picciani, P. H. S., Medeiros, E. S., Ribeiro, C., & Mattoso, L. H. C. (2012). Electrospinning of polymers in solution: part I: theoretical foundation. *Polímeros: Ciência e Tecnologia*, 22(2), 170-177. <http://dx.doi.org/10.1590/S0104-14282012005000026>.
 24. Gibson, P. W., Schreuder-Gibson, H. L., & Rivin, D. (1999). Electrospun fiber mats: transport properties. *AIChE Journal*, 45(1), 190-195. <http://dx.doi.org/10.1002/aic.690450116>.
 25. Agueda, J. R. S., Madrid, J., Mondragon, J. M., Lim, J., Tan, A., Wang, I., Duguran, N., & Bondoc, A. (2021). *Synthesis and characterization of electrospun Polyvinylidene Fluoride-based (PVDF) scaffolds for renal bioengineering*. In *International Conference on Biomedical Engineering - ICoBE 2021* (p. 012005). Bristol: IOP Publishing.
 26. Mercante, L. A., Andre, R. S., Macedo, J. B., Pavinatto, A., & Correa, D. S. (2021). Electrospun nanofibers and their applications: advances in the last decade. *Química Nova*, 44(6), 717-736.
 27. Alhassan, Z. A., Burezaq, Y. S., Nair, R., & Shehata, N. (2018). Polyvinylidene difluoride piezoelectric electrospun nanofibers: review in synthesis, fabrication, characterizations, and applications. *Journal of Nanomaterials*, 2018, 8164185. <http://dx.doi.org/10.1155/2018/8164185>.
 28. Costa, R. G. F., Oliveira, J. E., Paula, G. F., Picciani, P. H. S., Medeiros, E. S., Ribeiro, C., & Mattoso, L. H. C. (2012). Electrospinning of polymers in solution: part II: applications and perspectives. *Polímeros: Ciência e Tecnologia*, 22(2), 178-185. <http://dx.doi.org/10.1590/S0104-14282012005000018>.
 29. Kaspar, P., Sobola, D., Částková, K., Knápek, A., Burda, D., Orudzhev, F., Dallaev, R., Tofel, P., Trčka, T., Grmela, L., & Hadaš, Z. (2020). Characterization of Polyvinylidene Fluoride (PVDF) electrospun fibers doped by carbon flakes. *Polymers*, 12(12), 2766. <http://dx.doi.org/10.3390/polym12122766>. PMID:33255198.
 30. Sánchez, J. A. G., Furlan, R., López, R., Fachini, E., & Silva, A. N. R. (2014). *Piezoelectric effect in nanofibers deposited with magnetic field assisted electrospinning using solutions with PVDF and Fe₃O₄ nanoparticles*. In *29th Symposium on*

- Microelectronics Technology and Devices (SBMicro 2014)* (pp. 1-3). New York: IEEE.
31. Persano, L., Camposo, A., Tekmen, C., & Pisignano, D. (2013). Industrial upscaling of electrospinning and applications of polymer nanofibers: a review. *Macromolecular Materials and Engineering*, 298(5), 504-520. <http://dx.doi.org/10.1002/mame.201200290>.
 32. Bhardwaj, N., & Kundu, S. C. (2010). Electrospinning: a fascinating fiber fabrication technique. *Biotechnology Advances*, 28(3), 325-347. <http://dx.doi.org/10.1016/j.biotechadv.2010.01.004>. PMID:20100560.
 33. Gomes, D. S., Silva, A. N. R., Morimoto, N. I., Mendes, L. T. F., Furlan, R., & Ramos, I. (2007). Characterization of an electrospinning process using different PAN/DMF concentrations. *Polimeros: Ciência e Tecnologia*, 17(3), 206-211. <http://dx.doi.org/10.1590/S0104-14282007000300009>.
 34. Sengupta, D., Kottapalli, A. G. P., Chen, S. H., Miao, J. M., Kwok, C. Y., Triantafyllou, M. S., Warkiani, M. E., & Asadnia, M. (2017). Characterization of single polyvinylidene fluoride (PVDF) nanofiber for flow sensing applications. *AIP Advances*, 7(10), 105205. <http://dx.doi.org/10.1063/1.4994968>.
 35. Furlan, R., Rosado, J. A., & Silva, A. N. (2010). Study of formation of oriented fibers using injection of polymeric solutions inside electric fields defined by two parallel suspended electrodes. *ECS Transactions*, 31(1), 251-257. <http://dx.doi.org/10.1149/1.3474167>.
 36. Lima, R. R., Shimahara, A. I., Silva, A. N. R., & Silva, M. L. P. (2014). Arranjo simples e desmontável para a produção de nanofibras. *Boletim Técnico da Faculdade de Tecnologia de São Paulo*, 37, 971.
 37. Uchinokura, K., Sekine, T., & Matsuura, E. (1972). Raman scattering by silicon. *Solid State Communications*, 11(1), 47-49. [http://dx.doi.org/10.1016/0038-1098\(72\)91127-1](http://dx.doi.org/10.1016/0038-1098(72)91127-1).
 38. Du, X., Zhou, Z., Zhang, Z., Yao, L., Zhang, Q., & Yang, H. (2022). Porous, multi-layered piezoelectric composites based on highly oriented PZT/PVDF electrospinning fibers for high-performance piezoelectric nanogenerators. *Journal of Advanced Ceramics*, 11(2), 331-344. <http://dx.doi.org/10.1007/s40145-021-0537-3>.
 39. Fong, H., Chun, I., & Reneker, D. H. (1999). Beaded nanofibers formed during electrospinning. *Polymer*, 40(16), 4585-4592. [http://dx.doi.org/10.1016/S0032-3861\(99\)00068-3](http://dx.doi.org/10.1016/S0032-3861(99)00068-3).
 40. Sánchez, J. A. G., Furlan, R., Valle, R. L., Valle, P., & Silva, A. N. R. (2013). Influence of a magnetic field in the electrospinning of nanofibers using solutions with PVDF, DMF, acetone and Fe₃O₄ nanoparticles. In *28th Symposium on Microelectronics Technology and Devices (SBMicro 2013)* (pp. 1-3). New York: IEEE.
 41. Kim, N. K., Lin, R. J. T., Fakirov, S., Aw, K., & Bhattacharyya, D. (2014). Nanofibrillar Poly(vinylidene fluoride): preparation and functional properties. *International Journal of Polymeric Materials and Polymeric Biomaterials*, 63(1), 23-32. <http://dx.doi.org/10.1080/00914037.2013.769244>.
 42. Szewczyk, P. K., Gradys, A., Kim, S. K., Persano, L., Marzec, M., Kryshtal, A., Busolo, T., Toncelli, A., Pisignano, D., Bernasik, A., Kar-Narayan, S., Sajkiewicz, P., & Stachewicz, U. (2020). Enhanced piezoelectricity of electrospun polyvinylidene fluoride fibers for energy harvesting. *ACS Applied Materials & Interfaces*, 12(11), 13575-13583. <http://dx.doi.org/10.1021/acsaami.0c02578>. PMID:32090543.

Received: Dec. 21, 2022

Revised: Mar. 29, 2023

Accepted: Apr. 13, 2023